Polystyrene−Silica Colloidal Nanocomposite Particles Prepared by Alcoholic Dispersion Polymerization

Andreas Schmid, Syuji Fujii,† and Steven P. Armes*

Department of Chemistry, Dainton Building, The University of Sheffield, Brook Hill, Sheffield S3 7HF, United Kingdom

Carlos A. P. Leite and Fernando Galembeck

Universidade Estadual de Campinas, Instituto de Química, P. O. Box 6154, Campinas SP, São Paulo 13083-862, Brazil

Hideto Minami

Department of Chemical Science and Engineering, Faculty of Engineering, Kobe University, Kobe 657-8501, Japan

Naohiko Saito and Masayoshi Okubo

Division of Molecular Science, Graduate School of Science and Technology, Kobe University, Kobe 657-8501, Japan

Received September 27, 2006. Revised Manuscript Received February 5, 2007

Micrometer-sized silica-stabilized polystyrene latex particles and submicrometer-sized polystyrene−silica nanocomposite particles have been prepared by dispersion polymerization of styrene in alcoholic media in the presence of a commercial 13 or 22 nm alcoholic silica sol as the sole stabilizing agent. Micrometer-sized near-monodisperse silica-stabilized polystyrene latexes are obtained when the polymerization is initiated with a nonionic AIBN initiator. These particles are stabilized by silica particles that are present on the latex surface at submonolayer concentration. The total silica content is no greater than 1.1 wt %, which corresponds to a silica sol incorporation efficiency of less than 1.3%. Reduction of the initial silica sol concentration led to a systematic increase in the mean latex diameter. In contrast, submicrometer-sized polystyrene-silica nanocomposite particles are obtained when the polymerization is initiated with a cationic azo initiator. The silica contents of these nanocomposite particles are significantly higher, ranging up to 29 wt %. Zeta potential measurements, XPS, and electron spectroscopy imaging by transmission electron microscopy (ESI/TEM) studies reveal a well-defined core−shell morphology for these particles, whereby the core is polystyrene and the shell comprises the silica sol. After calcination, these nanocomposite particles can form hollow silica capsules. Variation of the initial silica sol and initiator concentration has relatively little effect on the final particle size and silica content of these polystyrene−silica nanocomposite particles, but indicates silica sol incorporation efficiencies up to 72%.

1. Introduction

The field of polymer nanocomposites is of rapidly growing interest.[1] It is well-known that the intimate mixing of polymers with either inorganic clays or silica on a nanometer scale can lead to (i) composite materials with superior mechanical properties and improved fire retardancy;[2−5] (ii) interesting building blocks for the fabrication of colloidal crystals;[6] and (iii) hollow polymeric particles for use in photonic crystals.[7] Recently, there has been increasing interest in the synthesis of colloidal nanocomposite particles.[8] Such syntheses typically involve either emulsion or dispersion polymerization,[9−21] although other techniques such as

* To whom correspondence should be addressed. E-mail: s.p.armes@sheffield.ac.uk.
† Current address: Department of Applied Chemistry, Osaka Institute of Technology, 5-16-1 Ohmiya, Asahi-ku, Osaka 535-8585, Japan.

(1) Percy, M. J.; Amalvy, J. I.; Randall, D. P.; Armes, S. P.; Greaves, S. J.; Watts, J. F. *Langmuir* **2004**, *20*, 2184.
(2) Gilman, J. W.; Jackson, C. L.; Morgan, A. B.; Harris, R.; Manias, E.; Giannelis, E. P.; Wuthenow, M.; Hilton, D.; Phillips, S. H. *Chem. Mater.* **2000**, *12*, 1866.
(3) Zhu, J.; Morgan, A. B.; Lamelas, F. J.; Wilkie, C. A. *Chem. Mater.* **2001**, *13*, 3774.
(4) Manias, E.; Touny, A.; Wu, L.; Strawhecker, K.; Lu, B.; Chung, T. C. *Chem. Mater.* **2001**, *13*, 3516.
(5) Kashiwagi, T.; Morgan, A. B.; Antonucci, J. M.; VanLandingham, M. R.; Harris, R. H.; Awad, W. H.; Shields, J. R. *J. Appl. Polym. Sci.* **2003**, *89*, 2072.
(6) Lu, Y.; McLellan, J.; Xia, Y. *Langmuir* **2004**, *20*, 3464.
(7) Xu, X.; Asher, S. A. *J. Am. Chem. Soc.* **2004**, *126*, 7940.
(8) Bourgeat-Lami, E. *J. Nanosci. Nanotechnol.* **2002**, *2*, 1.
(9) Bourgeat-Lami, E.; Lang, J. *J. Colloid Interface Sci.* **1998**, *197*, 293.
(10) Bourgeat-Lami, E.; Lang, J. *J. Colloid Interface Sci.* **1999**, *210*, 281.
(11) Bourgeat-Lami, E.; Lang, J. *Macromol. Symp.* **2000**, *151*, 377.
(12) Yoshinaga, K.; Yokoyama, T.; Sugawa, Y.; Karakawa, H.; Enomoto, N.; Nishida, H.; Komatsu, Michio. *Polym. Bull.* **1992**, *28*, 663.
(13) Luna-Xavier, J.-L.; Bourgeat-Lami, E.; Guyot, A. *Colloid Polym. Sci.* **2001**, *279*, 947.
(14) Luna-Xavier, J.-L.; Guyot, A.; Bourgeat-Lami, E. *J. Colloid Interface Sci.* **2002**, *250*, 82.

10.1021/cm062314c CCC: $37.00
Published on Web 04/21/2007

mini-emulsion polymerization[22−24] or the entrapment of preformed polymer during sol−gel processes have also been described.[25,26]

For example, Bourgeat-Lami et al.[9−11] encapsulated silica particles with diameters ranging between 13 and 629 nm within polystyrene via dispersion polymerization in aqueous ethanol in the presence of a poly(*N*-vinylpyrrolidone) or poly(styrene-*block*-ethylene oxide) stabilizer. Encapsulation only occurred when the silica particles were surface-functionalized by grafting 3-(trimethoxysilyl)propyl methacrylate (MPS) prior to polymerization. The resulting composite particles contained differing numbers of silica particles depending on the silica sol size; for silica sols of 450 nm diameter, only one silica particle was encapsulated per composite particle. Yoshinaga et al.[12] also encapsulated 470 nm silica particles by dispersion homopolymerization of styrene and methyl methacrylate using a cationic azobisisobutyramidine dihydrochloride (AIBA) initiator. Luna-Xavier et al.[13−15] prepared poly(methyl methacrylate)−silica (PMMA-SiO_2) nanocomposites via emulsion polymerization in the presence of a nonionic surfactant. Electrostatic adsorption of either the cationic AIBA initiator and/or the cationic end-groups of the polymer chains onto the anionic silica sol was shown to be essential for successful nanocomposite formation. Raspberry-like nanocomposite particles comprising polymer nodules surrounding a silica core were obtained when using smaller silica sols of 68 nm diameter. In contrast, larger silica sols led to well-defined core−shell morphologies. A cationic comonomer, 2-(methacryloyl) ethyltrimethylammnoium chloride, has been used by Chen et al.[27] to prepare raspberry-like PMMA-SiO_2 composite particles in the range of 180−576 nm utilizing 2−6 wt % cationic comonomer.

Armes and co-workers[16−18] prepared a wide range of nanocomposite particles by copolymerizing various vinyl monomers with 4-vinylpyridine (4VP) in the presence of an ultrafine aqueous silica sol. The presence of the basic 4VP auxiliary comonomer ensured strong interaction of the vinyl copolymers with the acidic silica surface, resulting in an attractive "surfactant-free" route to colloidally stable nanocomposites. Following a similar strategy, Chen et al.[19] prepared raspberry-like PMMA-SiO_2 nanocomposites using 1-vinylimidazole as an auxiliary comonomer. Recently Armes and co-workers reported that various commercial alcoholic silica sols of 13−22 nm diameter can be used to prepare either poly(3,4-ethylenedioxythiophene)-silica nanocomposite particles[20] or various vinyl polymer−silica nanocomposite particles[1,21] in an aqueous alcohol milieu in the absence of any comonomer auxiliary.

In two recent communications,[28,29] we have reported the application of dispersion polymerization in methanol or 2-propanol to prepare polystyrene−silica (PS−SiO_2) hybrid particles. Herein, we present a comprehensive investigation of these new composite particles. Improved silica incorporation efficiencies of up to 72% have been achieved, and additional techniques such as XPS and electron spectroscopy imaging in the TEM (ESI/TEM) are used to characterize these PS−SiO_2 hybrid particles. Furthermore, it is shown that calcination leads to hollow silica nanostructures that exhibit a blue coloration when placed on a dark background.

2. Experimental Section

2.1. Chemicals and Reagents. Styrene (Aldrich) was passed through a column of basic alumina to remove inhibitor and then stored at −20 °C prior to use. 2,2′-Azobis(isobutyramidine) dihydrochloride (AIBA; Aldrich), 4,4′-azobis(4-cyanovaleric acid) (ACVA; Acros), 2,2′-azobisisobutyronitrile (AIBN; BDH), methanol, and 2-propanol (both ex. Fisher Scientific) were all used as received. Three commercial alcoholic silica sols were obtained from Nissan Chemicals (Texas): MT-ST (13 nm silica sol in methanol at 30 wt %, viscosity 1.5 mPa s), MA-ST (22 nm silica sol in methanol at 30 wt %, viscosity 2.2 mPa s), and IPA-ST (13 nm silica sol in 2-propanol at 30 wt %, viscosity 5.8 mPa s); each alcoholic sol was used as received.

2.2. Particle Synthesis. A typical synthesis was carried out as follows. Styrene monomer (2.50 mL), the appropriate alcoholic silica sol (6.67 g, which corresponds to 2.0 g dry silica), and depending on the silica sol that is used, either methanol or 2-propanol (19.0 mL) were added at 25 °C in turn to a round-bottomed flask equipped with a nitrogen gas inlet, a condenser, and a magnetic stir bar. Twenty-three milligrams of the appropriate initiator (1.0 wt % based on styrene) was added and the reaction mixture was degassed with nitrogen prior to immersion in a 60 °C oil bath under a nitrogen blanket and stirred for 24 h. Monomer conversions were determined gravimetrically and were usually at least 90%. However, somewhat lower conversions were achieved for two experiments conducted at lower initiator concentrations (70−80%). The resulting milky white colloidal dispersions were purified by eight centrifugation−redispersion cycles (3000 rpm), with each successive supernatant being carefully decanted and replaced, as follows. Initially, the supernatant was replaced three times with pure methanol (or 2-propanol), and then with mixtures of the alcohol and deionized water (2:1, 1:1, and 1:2); it was finally replaced twice with deionized water. Excessive centrifugation rates (>8000 rpm) and times (>1 h) were avoided, because these would otherwise result in sedimentation of the excess silica sol and make redispersion of the sedimented particles more difficult. Dynamic light scattering and TEM studies confirmed that the particle size and morphology were not affected by this purification protocol, (data not shown).

3. Particle Characterization

3.1. Particle Size. Particle diameters were determined by disk centrifuge photosedimentometry (DCP; Brookhaven Instruments) which reports weight-average particle size

(15) Luna-Xavier, J.-L.; Guyot, A.; Bourgeat-Lami, E. *Polym. Int.* **2004**, *53*, 609.
(16) Barthet, C.; Hickey, A. J.; Cairns, D. B.; Armes, S. P. *Adv. Mater.* **1999**, *11*, 408.
(17) Percy, M. J.; Barthet, C.; Lobb, J. C.; Khan, M. A.; Lascelles, S. F.; Vamvakaki, M.; Armes, S. P. *Langmuir* **2000**, *16*, 6913.
(18) Amalvy, J. I.; Percy, M. J.; Armes, S. P.; Wiese, H. *Langmuir* **2001**, *17*, 4770.
(19) Chen, M.; Wu, L.; Zhou, S.; You, B. *Macromolecules* **2004**, *37*, 9613.
(20) Han, M. G.; Armes, S. P. *Langmuir* **2003**, *19*, 4523.
(21) Percy, M. J.; Armes, S. P. *Langmuir* **2002**, *18*, 4562.
(22) Tiarks, F.; Landfester, K.; Antonietti, M. *Langmuir* **2001**, *17*, 5775.
(23) Zhou, J.; Zhang, S.; Qiao, X.; Li, X.; Wu, L. *J. Polym. Sci., Part A: Polym. Chem.* **2006**, *44*, 3202.
(24) Antonietti, M.; Landfester, K. *Prog. Polym. Sci.* **2002**, *27*, 689.
(25) Sertchook, H.; Avnir, D. *Chem. Mater.* **2003**, *15*, 1690.
(26) Sertchook, H.; Elimelech, H.; Avnir, D. *Chem. Mater.* **2005**, *17*, 4711.
(27) Chen, M.; Zhou, S.; You, B.; Wu, L. *Macromolecules* **2005**, *38*, 6411.
(28) Schmid, A.; Fujii, S.; Armes, S. P. *Langmuir* **2005**, *21*, 8103.
(29) Schmid, A.; Fujii, S.; Armes, S. P. *Langmuir* **2006**, *22*, 4923.

distributions of the purified aqueous latexes. Solid-state particle densities were measured by helium pycnometry (Micromeritics AccuPyc 1330 instrument).

3.2. Particle Morphology. Particle morphologies were determined by transmission electron microscopy (TEM). TEM studies were conducted using a Philips CM 100 instrument operated at 100 kV. Ten microliters of the purified latex sample was dried on a carbon-coated copper grid. SEM studies were performed on a JEOL JSM 6400 scanning electron microscope. Samples were dried on adhesive carbon disks and sputter-coated with a thin layer of gold prior to examination.

For hydrofluoric acid (HF) etching experiments, the protocol described by Han and Armes[30] was followed. The aqueous latex (5.0 mL) was stirred for 2 h with 40 mL of 20 wt % aqueous HF. It was centrifuged and redispersed in water repeatedly until the supernatant had acquired a neutral pH.

Ultramicrotomy and ESI/TEM: The nanomorphology and the spatial elemental distribution within the polystyrene-silica nanocomposite particles were assessed by ESI using a Carl Zeiss CEM 902 transmission electron microscope equipped with a Castaing−Henry−Ottensmeyer filter spectrometer within the column. The nanocomposite particle dispersions were dried at room temperature under air and the resulting solids were embedded in a soft epoxy resin that was cured for 24 h at room temperature, followed by 24 h in an oven at 60 °C. The resin blocks were trimmed and cut in an EM FC6 Leica ultramicrotome using a Diatome diamond knife. 40-nm ultrathin sections were collected over copper grids for ESI/TEM analysis. Images were acquired using electrons with element-specific threshold energies, 101 eV for silicon, and 284 eV for carbon, recorded using a slow-scan CCD camera (Proscan), and processed using AnalySis 3.0 software. A more detailed description of an ESI/TEM study on related nanocomposite particles has been recently published.[31]

3.3. Silica Content. Thermogravimetric analyses (TGA) were performed using a Perkin-Elmer Pyris 1 TGA instrument. Dried samples were heated in air to 800 °C at a heating rate of 10 °C min^{-1}, and the observed mass loss was attributed to the quantitative pyrolysis of the polystyrene, with the remaining incombustible residues assumed to be pure silica (SiO_2).

3.4. Surface Analysis. Aqueous electrophoresis measurements were performed in 1 mM KCl solution using a Malvern Zetasizer NanoZS instrument. The solution pH was adjusted by the addition of HCl or KOH.

X-ray photoelectron spectroscopy data were obtained with a Shimadzu ESCA-3400 apparatus using magnesium Kα radiation (1253.6 eV) at a potential of 10 kV and an X-ray current of 20 mA. The pressure in the measurement chamber was ca. 8.0×10^{-7} Pa. A Digital Equipment Corporation DS-800 computer system was used for spectrometer control and data handling. Dried particles were stored under reduced pressure by continuous operation of a rotary pump just before XPS measurement. The dried particles were spread on an indium plate with a spatula.

(30) Han, M. G.; Armes, S. P. *J. Colloid Interface Sci.* **2003**, *262*, 418.
(31) Amalvy, J. I.; Percy, M. J.; Armes, S. P.; Leite, C. A. P.; Galembeck, F. *Langmuir* **2005**, *21*, 1175.

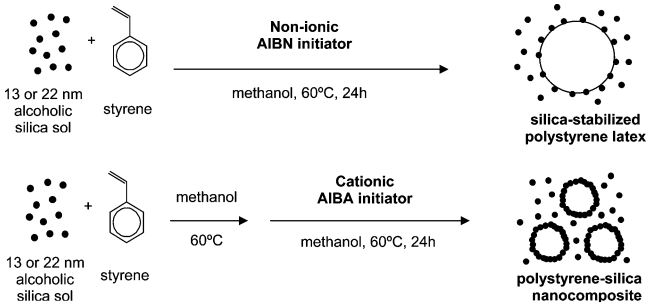

Figure 1. Schematic representation of the experimental protocols used for the preparation of silica-stabilized polystyrene latex particles (top) and polystyrene−silica nanocomposite particles (bottom) by alcoholic dispersion polymerization using ultrafine commercial alcoholic silica sols and either nonionic AIBN or cationic AIBA azo initiators.

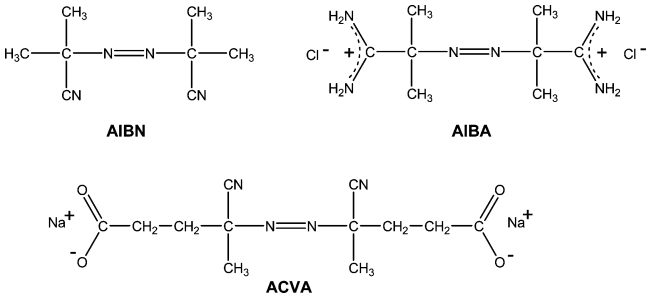

Figure 2. Chemical structures of the three initiators used for the dispersion polymerization of styrene in alcoholic media in the presence of commercial alcoholic silica sols.

3.5. Adsorption of AIBA onto Silica Sol. The adsorption isotherm of the cationic AIBA initiator on the 22 nm methanolic silic sol was determined using the depletion method. Mixtures of 1.33 g of MA-ST silica sol (400 mg dry silica) in 40 mL of methanol containing varied amounts of AIBA initiator were equilibrated at room temperature for 30 min and then centrifuged at 20 000 rpm for 3 h. The AIBA concentrations in the supernatants were determined by UV−visible spectroscopy using the absorption at 368 nm and a previously constructed calibration curve.

3.6. Calcination Experiments. Calcination of samples prior to TEM studies was performed as follows. A drop of a diluted latex dispersion was dried onto a carbon-coated copper grid. The grid was then heated in the TGA pan under air up to 550 °C at a heating rate of 10 °C per min. This temperature was chosen to completely pyrolyse the polystyrene cores but to leave the TEM grid still useable for subsequent TEM studies. Bulk samples were obtained by heating selected nanocomposites in air up to 800 °C at 10 °C min^{-1}.

4. Results and Discussion

Dispersion polymerization of styrene was conducted in either methanol or 2-propanol using commercial alcoholic silica sols as the sole stabilizing agent; an overview of the experimental protocol is shown in Figure 1. The polymerization was initiated using three different azo initiators (Figure 2), nonionic 2,2′azobisisobutyronitrile (AIBN), cationic 2,2′azobis(isobutyramidine) dihydrochloride (AIBA), and anionic 4,4′azobis(4-cyanovaleric acid) (ACVA). Depending on the type of initiator used, different particle sizes and morphologies were obtained.

Table 1. Effect of Varying the Silica Sol Type, Particle Diameter, and Concentration on the Mean Particle Diameter and Silica Content of Silica-Stabilized Polystyrene Latex Particles Produced via Alcoholic Dispersion Polymerization at 60 °C Using the Nonionic AIBN Initiator

entry no.	silica sol type[a]	silica sol concn (w/v %)	solvent type	silica content[b] (wt %)	silica sol incorporation efficiency (%)	particle density[c] (g cm^{-3})	particle diameter[d] D_w (μm)
1	MT-ST	8.0	methanol	0.7	0.8	1.07	1.36 ± 0.12
2	MT-ST	4.0	methanol	0.1	0.2	1.07	2.50 ± 0.36
3	MT-ST	2.0	methanol	<0.1	0.4	1.07	3.10 ± 0.34
4	MA-ST	8.0	methanol	1.1	1.3	1.07	1.22 ± 0.11
5	MA-ST	4.0	methanol	0.5	1.1	1.06	1.64 ± 0.21
6	MA-ST	2.0	methanol	0.3	1.4	1.06	1.91 ± 0.29
7	IPA-ST	8.0	2-propanol	0.7	0.8	1.07	3.26 ± 0.49
8	none	n/a	methanol	n/a	n/a	1.05	n/a
9	none	n/a	2-propanol	n/a	n/a	1.05	n/a

[a] IPA-ST, 13 nm silica sol in 2-propanol at 30 wt %; MA-ST, 22 nm silica sol in methanol at 30 wt %; MT-ST, 13 nm silica sol in methanol at 30 wt %. The silica sol concentration was 8.0 w/v % based on total volume. [b] Determined from thermogravimetric analysis assuming that the incombustible residues were SiO_2. [c] As measured by helium pycnometry. [d] Weight-average diameter ± standard deviations of the redispersed, purified particles as determined by disk centrifuge photosedimentomety.

Table 2. Effect of Varying the Silica Sol Type and Silica Sol Particle Diameter on the Mean Particle Diameter and Silica Content of Polystyrene−Silica Nanocomposite Particles Produced via Alcoholic Dispersion Polymerization at 60 °C Using a Cationic AIBA Initiator; Various Control Experiments Are Also Included (entries 12−15).

entry no.	silica sol type[a]	solvent	initiator type	initiator amount (mg/g_{SiO2})	temperature for initiator addition (°C)	silica content[b] (wt %)	silica sol incorporation efficiency (%)	particle density[c] (g cm^{-3})	particle diameter[d] D_w (nm)
1	MT-ST	methanol	AIBA	11.5	25[j]	22	32	1.20	420 ± 40
2	MT-ST	methanol	AIBA	11.5	25[k]	29	46	1.25	374 ± 42
3	MT-ST	methanol	AIBA	11.5	60	26	40	1.24	331 ± 43
4	MA-ST	methanol	AIBA	11.5	60	18	25	1.16	362 ± 22
5	IPA-ST	2-propanol	AIBA	11.5	60	13	17	1.14	464 ± 45
6	MA-ST	methanol	AIBA[e]	1.5	60	21	30	1.20	262 ± 125
7	MA-ST	methanol	AIBA[f]	3.3	60	24	37	1.23	326 ± 59
8	MA-ST[g]	methanol	AIBA	5.7	60	25	19	1.24	322 ± 36
9	MA-ST[h]	methanol	AIBA	3.8	60	24	12	1.24	335 ± 28
10	MA-ST[i]	methanol	AIBA	23.0	60	24	72	1.23	354 ± 43
11	MT−ST	methanol	ACVA	11.5	25	precipitation			
12	none	methanol	AIBA	as in entry 1	25	n/a	n/a	1.05	760 ± 50
13	none	methanol	ACVA	as in entry 1	25	n/a	n/a	1.05	967 ± 16
14	none	2-propanol	AIBA	as in entry 1	25	n/a	precipitation		
15	none	2-propanol	ACVA	as in entry 1	25	n/a	precipitation		

[a] IPA-ST, 13 nm silica sol in 2-propanol at 30 wt %; MA-ST, 22 nm silica sol in methanol at 30 wt %; MT−ST, 13 nm silica sol in methanol at 30 wt %. The silica sol concentration was 8.0 w/v% based on total volume. [b] Determined from thermogravimetric analysis assuming that the incombustible residues were SiO_2. [c] As measured by helium pycnometry. [d] Weight-average diameter ± standard deviation of the redispersed, purified particles as determined by disk centrifuge photosedimentomety. [e] Initiator concentration = 0.13 wt % based on styrene. [f] Initiator concentration = 0.29 wt % based on styrene. [g] Silica sol concentration = 16 w/v %. [h] Silica sol concentration = 24 w/v %. [i] Silica sol concentration = 4 w/v %. [j] Initiator added first. [k] Initiator added second.

4.1. Micrometer-Sized Silica-Stabilized Polystyrene Latex Particles (AIBN initiator). AIBN initiation of the dispersion polymerization of styrene in either methanol or 2-propanol in the presence of any of the three commercial alcoholic silica sols as the sole stabilizer led to the formation of well-defined polystyrene latex particles.[28] The effects of varying the silica sol diameter, silica sol concentration, and silica sol type on the latex particle diameter, particle density, and silica content are summarized in Table 1.

4.1.1. Influence of the Silica Sol Type. Polymerizations were conducted in methanol in the presence of a 13 or 22 nm silica sol dispersed in methanol and in 2-propanol in the presence of a 13 nm silica sol dispersed in 2-propanol. Figure 3 shows electron microscopy images of the particles obtained using each of the three silica sols. Narrow particle size distributions were obtained in both cases in methanol, whereas the particles obtained in 2-propanol had a somewhat broader particle size distribution. DCP analysis, also shown in Figure 3, confirmed narrow particle size distributions for the two polymerizations carried out in methanol, with mean particle diameters of 1.4 μm for the 13 nm silica sol (entry 1 in Table 1 and Figure 3a) and 1.2 μm for the 22 nm silica sol (entry 4 in Table 1 and Figure 3b), respectively. The particles prepared in 2-propanol using the 13 nm silica sol had a mean diameter of 3.3 μm (see entry 7 in Table 1 and Figure 3c). These differences in size and polydispersity are presumably related to the different degrees of solubility of the growing polymer chains in methanol and 2-propanol. The critical chain length for precipitation is shorter in the more polar methanol, leading to smaller particles. In 2-propanol, longer polymer chains are solubilized, leading to the larger particles and a broader size distribution. Another important parameter is likely to be the dielectric constant of the continuous phase: both Lok and Ober and also Dawkins and co-workers reported that larger polystyrene latexes were obtained using less polar solvents in dispersion polymerization syntheses.[32,33] On close inspection, the "patchy" distribution of the silica sol on the latex particle surface is clearly visible by TEM (see Figure 6).

Latex densities were around 1.07 g cm^{-3} and thus fairly close to that of pure polystyrene (1.05 g cm^{-3}). This

(32) Lok, K. P.; Ober, C. K. *Can. J. Chem.* **1985**, *63*, 209.
(33) Dawkins, J. V.; Neep, D. J.; Shaw, P. L. *Polymer* **1994**, *35*, 5366.

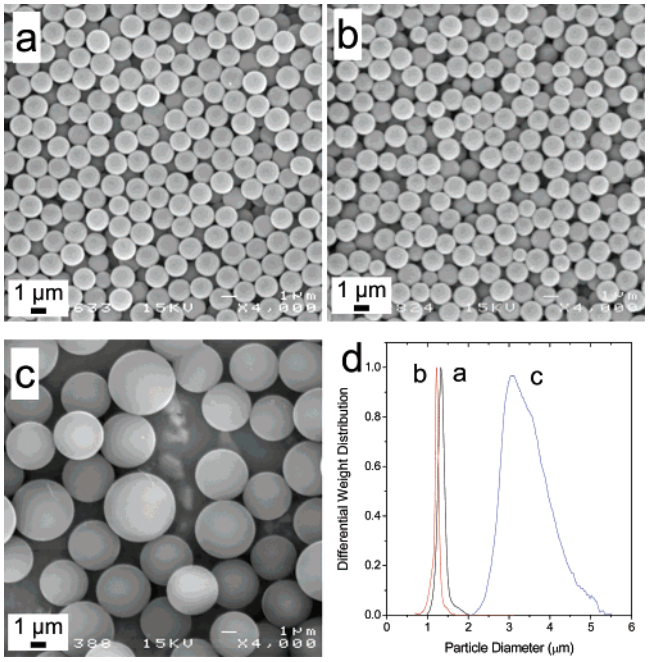

Figure 3. Scanning electron microscopy images of silica-stabilized polystyrene latex particles prepared via alcoholic dispersion polymerization initiated with AIBN (a) in the presence of a MT-ST 13 nm silica sol in methanol (entry 1 in Table 1), (b) a MA-ST 22 nm silica sol in methanol (entry 4 in Table 1), and (c) a IPA-ST 13 nm silica sol in 2-propanol (entry 7 in Table 1). Disk centrifuge studies of these silica-stabilized polystyrene latex particles show the respective weight-average particle size distributions in (d).

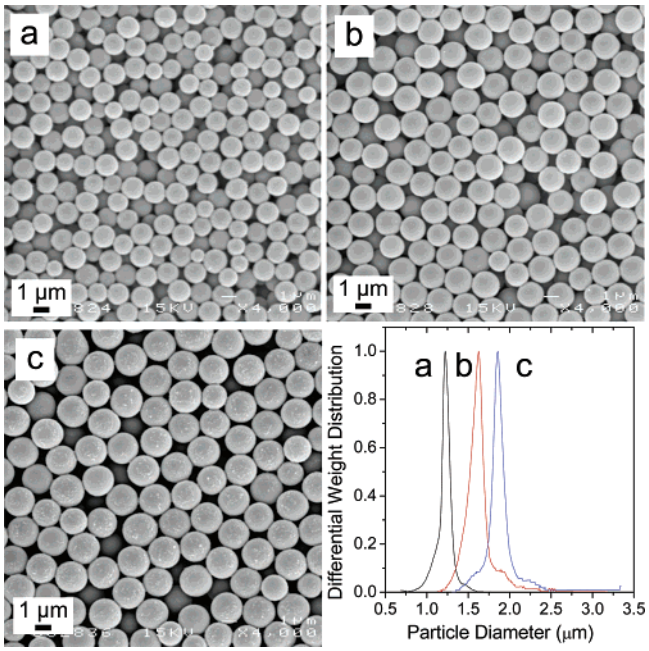

Figure 4. SEM images of silica-stabilized polystyrene latex particles prepared via alcoholic dispersion polymerization initiated with AIBN in presence of the 22 nm MA-ST silica sol at different silica sol concentrations: (a) 8.0 w/v% (entry 4 in Table 1), (b) 4.0 w/v% (entry 5 in Table 1), and (c) 2.0 w/v% (entry 6 in Table 1), as well as the corresponding disk centrifuge particle size distribution curves.

suggested that the silica contents of these polystyrene particles were very low. This was confirmed by thermogravimetric studies, which revealed silica contents between 0.7 and 1.1 wt % (see Table 1, entries 1, 4, and 7).

4.1.2. Influence of the Silica Sol Concentration. For the conventional dispersion polymerization of styrene in alcoholic media in the presence of poly(*N*-vinylpyrolidone), it has been previously shown that larger polystyrene latexes are obtained at lower stabilizer concentrations.[34] A similar stabilizer effect on particle diameter was observed for the alcoholic silica sols used in the present study. For example, decreasing the concentration of the 22 nm silica sol from 8.0 w/v % to 2.0 w/v % (entries 4−6 in Table 1) led to a systematic increase in the mean latex diameter from 1.2 to 1.9 μm, see Figure 4. Similarly, the mean particle diameter increased from 1.4 to 3.1 μm for the 13 nm silica sol (entries 1−3 in Table 1) under the same conditions. These observations support the hypothesis that the silica sol acts as a stabilizer in these formulations.

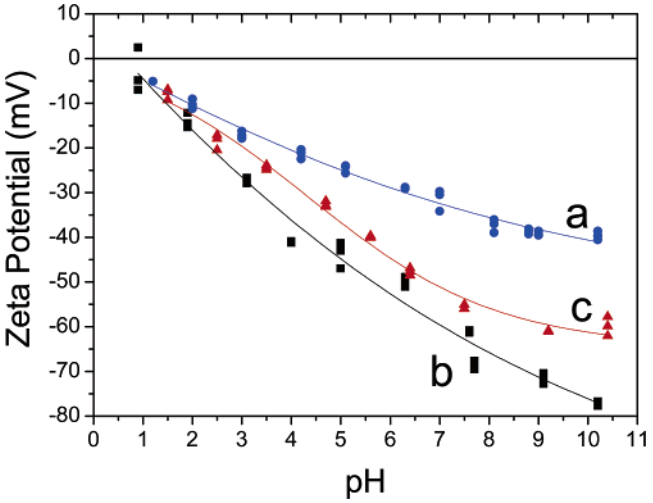

Figure 5. Aqueous electrophoresis curves obtained for (a) the MA-ST 22 nm pristine commercial alcoholic silica sol, (b) the silica-stabilized polystyrene latex particles prepared with AIBN in presence of the same silica sol (entry 4 in Table 1) and (c) the polystyrene−silica nanocomposite prepared with the cationic AIBA initiator using this silica sol (entry 4 in Table 2).

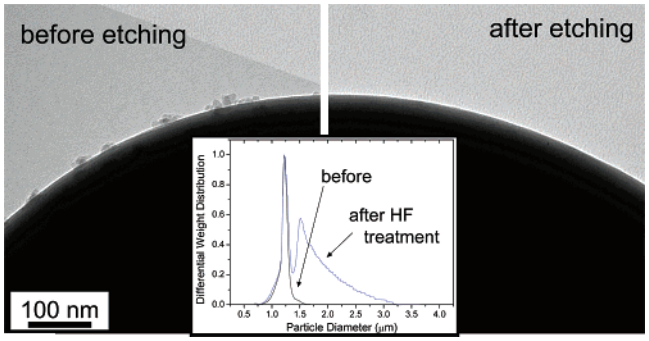

Figure 6. TEM image of a silica-stabilized polystyrene latex particle prepared via alcoholic dispersion polymerization initiated with AIBN in presence of a 22 nm MA-ST silica sol (entry 4 in Table 1) before (left) and after (right) treatment with HF. Note the disappearance of the silica sol during this process. The inset shows the DCP curves of the particles before and after HF etching, with visible flocculation occurring when the silica sol is removed.

4.1.3. Colloidal Stability. Aqueous electrophoresis studies indicate that these latexes possess anionic surface charge over a wide pH range, similar to the pristine alcoholic silica sols, see Figure 5. This suggests that the silica sol is adsorbed at the surface of the latex particles. Thus these latexes can be considered to be charge-stabilized, albeit by highly localized

(34) Paine, A. J.; Luymes, W.; McNulty, J. *Macromolecules* **1990**, *23*, 3104.

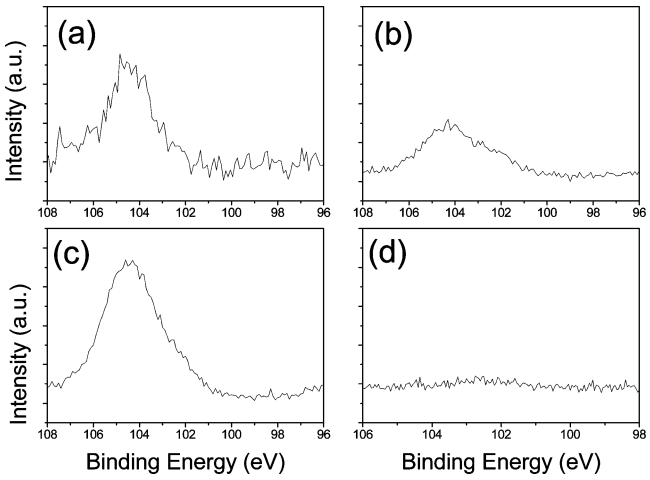

Figure 7. XPS Si2p core-line spectra of silica-stabilized polystyrene latex particles prepared via alcoholic dispersion polymerization initiated with AIBN in the presence of three different alcoholic silica sols: (a) 13 nm IPA-ST silica sol in 2-propanol (entry 7 in Table 1), (b) 13 nm MA-ST silica sol in methanol (entry 1 in Table 1), (c) 22 nm MA-ST silica sol in methanol (entry 4 in Table 1), and (d) polystyrene prepared in the absence of any silica sol (entry 8 in Table 1).

13 or 22 nm domains of ionized silanol groups (because the hydrophobic AIBN initiator confers no ionic charge). Moreover, HF etching experiments on these silica-stabilized latex particles led to complete digestion of the silica sol, see Figure 6. The loss in colloidal stability of these HF-treated latex particles led to their weak flocculation, as indicated by disk centrifuge studies and confirmed by visual inspection.

In addition to the TEM and zeta potential measurements, which suggested that the silica particles are located at the latex surface, XPS analysis (Figure 7) confirmed the surface presence of the silica sol. Thus, weak Si2p signals were visible for latex particles prepared in the presence of the silica sol, but no Si2p signal was detected in precipitated polystyrene obtained in the absence of any silica sol. Comparison of the surface Si/C atomic ratios calculated from the XPS data (see entries 4−6 in Table 3) with the corresponding bulk Si/C atomic ratios suggests that most, if not all, of the silica sol is located at the latex surface. Moreover, comparing the surface silicon atomic percent contents with that of the corresponding silica sol (see entries 1−3 in Table 3) allows estimation of the approximate surface concentration of the silica sol, which ranges from 2.3 to 15%. This suggests that the latex surface is dominated by the polystyrene component, with the silica sol being present at only submonolayer coverage. This interpretation is consistent with our TEM observations.

Although their surface concentration is low, the surface charge conferred by the surface-adsorbed silica particles is essential for the colloidal stability of these polystyrene latex particles. In this context, it is perhaps noteworthy that Horozov et al.[35,36] have also invoked charge stabilization to explain the long-range ordering of silica particles adsorbed at submonolayer coverage at a planar oil−water interface.

4.1.4. Control Experiments. Two important control experiments were also conducted. Styrene was polymerized in either methanol or 2-propanol after initiation with AIBN at 60 °C. In both cases, a macroscopic precipitate of polystyrene was obtained with no evidence for any colloidal particles.

It is clear that the stabilizer efficiency of these alcoholic silica sols is very low, as only approximately 1% of the silica sol actually gets incorporated into the polystyrene latex particles, as calculated from thermogravimetric measurements. However, it is emphasized that the presence of the silica sol is absolutely essential for successful latex syntheses. The actual mechanism of the silica incorporation remains uncertain. A π-electron interaction between the aromatic ring of the polymerized styrene residues and the silica surface has been suggested by Agarwal et al.[37] on the basis of ^{13}C solid-state NMR studies using magic angle spinning. We tentatively suggest that such an interaction is also likely to be important for the formation of the silica-stabilized polystyrene latex particles. However, similar NMR studies are unlikely to be successful in the present case because of the relatively low silica contents of these new particles.

The polystyrene components of the silica-stabilized polystyrene latexes were extracted by dissolution in THF, followed by centrifugation to remove the silica particles. GPC analyses of these polystyrene samples are shown in the Supporting Information (see Figure S3). The weight-average molecular weight (M_w) of the polystyrene precipitate prepared in the absence of any silica sol was significantly lower than that obtained for the corresponding polystyrene prepared in colloidal form (34 000 vs 107 000 for the methanol syntheses and 58 000 vs 308 000 for the 2-propanol syntheses). Similar results have been reported in the literature for other dispersion polymerization syntheses.[38]

4.2. Submicrometer-Sized Polystyrene−Silica Nanocomposite Particles (AIBA initiator). In contrast to the silica-stabilized polystyrene latex particles obtained using the nonionic AIBN initiator, submicrometer-sized polystyrene−silica nanocomposite particles were obtained using a cationic AIBA initiator.[29] The effects of varying the silica sol diameter, silica sol concentration, and silica sol type on the nanocomposite particle diameter, particle density, and silica content are summarized in Table 2.

4.2.1. Influence of Initiator Addition. In principle, there are at least three methods for carrying out these nanocomposite particle syntheses. Method A involves dissolving the AIBA initiator first in part of the methanol, then adding the silica sol and the styrene monomer with subsequent heating to the desired reaction temperature (entry 1 in Table 2). Method B involves diluting the silica sol with most of the methanol, adding the styrene monomer, and then adding the initiator dissolved in the remaining methanol with subsequent heating to the reaction temperature (entry 2 in Table 2). Method C involves dilution of the silica sol with most of the methanol, addition of the styrene monomer, then heating to the reaction temperature of 60 °C with subsequent addition of the AIBA initiator dissolved in the remaining methanol (entry 3 in Table 2). Thus, methods A,

(35) Horozov, T. S.; Binks, B. P. *Colloids Surf., A* **2005**, *267*, 64.
(36) Horozov, T. S.; Aveyard, R.; Binks, B. P.; Clint, J. H. *Langmuir* **2005**, *21*, 7405.
(37) Agarwal, G. K.; Titman, J. J.; Percy, M. J.; Armes, S. P. *J. Phys. Chem. B* **2003**, *107*, 12497.
(38) Canelas, D. A.; Betts, D. E.; DeSimone, J. M. *Macromolecules* **1996**, *29*, 2818.

Table 3. Comparison of Bulk and Surface Compositions for a Silica Sol Reference Material, Three Silica-Stabilized Polystyrene Latexes, and Three Polystyrene−Silica Nanocomposites, as Calculated from Combined Thermogravimetric Analyses and XPS Studies

			bulk composition (TGA)			surface composition (XPS)		
entry no.	silica sol diameter, solvent	initiator type	Si at %	C at %	bulk atomic ratio Si/C	Si at %	C at %	surface atomic ratio Si/C
1	13 nm, methanol		29[a]	0.4[b]	72.5	39	2.4	15.8
2	22 nm, methanol		29[a]	0.2[b]	145	35	5.5	6.4
3	13 nm, 2-propanol		29[a]	2.0[b]	14.5	39	1.9	20.5
4	13 nm, methanol	AIBN	0.076	49.9	0.0015	2.5	86	0.03
5	22 nm, methanol	AIBN	0.12	49.8	0.0024	5.4	79	0.07
6	13 nm, 2-propanol	AIBN	0.076	49.9	0.0015	0.91	95	0.01
7	13 nm, methanol	AIBA	3.41	44.9	0.076	26	26	1.0
8	22 nm, methanol	AIBA	2.22	46.7	0.048	15	38	0.40
9	13 nm, 2-propanol	AIBA	1.54	47.7	0.032	17	38	0.45

[a] Estimated by allowing for surface moisture and assuming that the TGA residue is SiO_2. [b] Determined from carbon microanalysis.

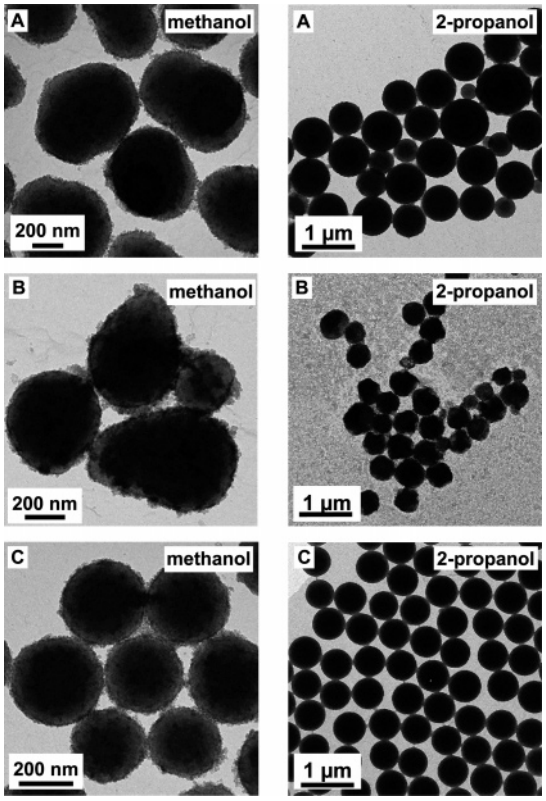

Figure 8. TEM images of polystyrene−silica nanocomposites prepared by dispersion polymerization in methanol (left) or 2-propanol (right) initiated with AIBA in the presence of a 13 nm silica sol. The method of initiator addition was varied as follows: AIBA added (A) before the silica sol at 25 °C, (B) after the silica sol at 25 °C, and (C) after the reaction mixture was heated to 60 °C. Methods A and B led to particles with either ill-defined morphologies or broad polydispersities, whereas method C produced well-defined spherical particles with narrow polydispersities.

B, and C essentially differ in the timing of the initiator addition. AIBA is added first at 25 °C prior to the addition of the silica sol (method A), added after the silica sol at 25 °C (method B), or after the reaction mixture is already heated to 60 °C (method C).

These three modes of initiator addition were studied using the 13 nm silica sols dispersed in either methanol or 2-propanol at a constant silica sol concentration of 8.0 w/v %. The TEM images of the resulting particles are shown in Figure 8. They are rather similar in size, regardless of the mode of initiator addition. However, there is a distinct difference in particle morphology. For methods A and B (in which the initiator is added at 25 °C), the particles either have a somewhat ill-defined, non-spherical morphology or have a broad size distribution. For method C, where the initiator is added last at 60 °C, the particles are distinctly more spherical. These empirical observations are somewhat perplexing, particularly in view of the fact that the cationic AIBA initiator is adsorbed onto the silica sol (see later). In this context, it might be supposed that surface polymerization is important for successful nanocomposite particle formation and that therefore method C would be the *least* beneficial for the preparation of well-defined particles. However, this hypothesis does not seem to agree with the experimental observations. Clearly, our understanding of the particle formation mechanism in these syntheses requires substantial refinement. One reviewer suggested that, because the AIBA initiator was added at room temperature in methods A and B, some decomposition might occur below 60 °C (i.e., during the heating stage), which may influence the observed particle morphology. According to its manufacturer, the half-life of this initiator is approximately 500 h at 30 °C, 100 h at 40 °C, 21 h at 50 °C, and 7 h at 60 °C, so it is certainly feasible that a small amount of polymer is formed during the heating stage. However, it takes only around 30 min to heat the reaction vessel up to 60 °C, which suggests that the extent of polymerization below this temperature is likely to be rather low. It is also noteworthy that the TEM images suggest much higher silica sol surface concentrations for all three methods A−C, at least compared to the silica-stabilized polystyrene latexes obtained with the AIBN initiator. These observations were confirmed by TGA studies (see below).

4.2.2. Influence of Silica Sol Type. Addition of the AIBA initiator after the reaction mixture is heated to 60 °C leads to approximately spherical nanocomposite particles. This method was then applied to all three alcoholic silica sols (MT-ST, 13 nm silica sol in methanol; MA-ST, 22 nm silica sol in methanol; IPA-ST, 13 nm silica sol in 2-propanol), which in all cases led to the formation of spherical polystyrene−silica nanocomposite particles as shown in Figure 9. Mean particle diameters of 331 ± 43 nm for the 13 nm silica sol in methanol (entry 3 in Table 2), 362 ± 22 nm for the 22 nm silica sol in methanol (entry 4 in Table 2), and 464 ± 45 nm for the 13 nm silica sol in 2-propanol (entry 5 in Table 2) were obtained by DCP measurements, which suggests relatively narrow size distributions. Like the silica-stabilized polystyrene latex particles, nanocomposite syntheses conducted in the less polar 2-propanol also led to larger particles than those obtained in the more polar methanol.

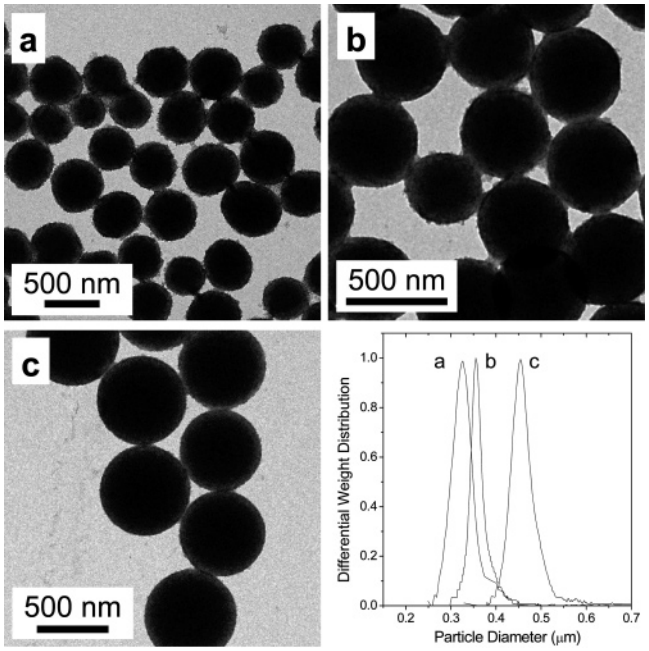

Figure 9. TEM images of polystyrene−silica nanocomposites prepared via alcoholic dispersion polymerization initiated with AIBA. Three different silica sols were used: (a) 13 nm MT−ST silica sol in methanol (entry 3 in Table 2), (b) 22 nm MA-ST silica sol in methanol (entry 4 in Table 2), and (c) 13 nm IPA-ST silica sol in 2-propanol (entry 5 in Table 2). The disk centrifuge data show the weight-average particle size distributions of these three different types of nanocomposite particles.

Nanocomposite densities ranged from 1.14 to 1.24 g cm^{-3}, which are significantly higher than that of pure polystyrene (1.05 g cm^{-3}). Assuming additivity, and taking the mean density of the silica sols to be 2.15 g cm^{-3}, these nanocomposite densities indicated approximately silica contents ranging from 15 to 29 wt %. Thermogravimetric analysis confirmed silica contents of 26 wt % (entry 3 in Table 2) for nanocomposites prepared with the 13 nm silica sol in methanol, 18 wt % (entry 4 in Table 2) for nanocomposites prepared with the 22 nm silica sol in methanol, and 13 wt % (entry 5 in Table 2) for nanocomposites prepared with the 13 nm silica sol in 2-propanol. These silica contents correspond to silica incorporation efficiencies of up to 40% for nanocomposites prepared with the 13 nm methanolic silica sol but only 17% for the particles prepared with the 13 nm silica sol in 2-propanol. Given their relatively high silica contents, these particles can be described as genuine polystyrene−silica nanocomposites. Moreover, taking into account the imperfect 2D packing of small spheres around a larger sphere, these silica contents are approximately those expected for monolayer coverage and hence a core−shell morphology. This interpretation is fully consistent with our ESI/TEM studies of ultramicrotomed polystyrene−silica nanocomposite particles, see later.

As the choice of initiator is the only difference in the synthesis protocol, it is likely that electrostatic attraction between the cationic initiator and the anionic silica sol promotes successful nanocomposite formation; this explanation was also offered by Luna-Xavier et al.[13,14] To test this hypothesis, the extent of adsorption of the cationic AIBA initiator from methanol onto the 22 nm methanolic silica sol at room temperature was determined by the depletion method using UV−visible absorption spectrometry to monitor the

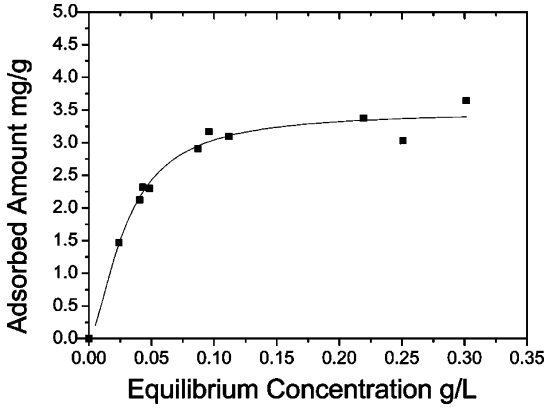

Figure 10. Langmuir-type isotherm of the cationic AIBA initiator adsorbed onto 22 nm MA-ST silica sol in methanol, determined by the depletion method (using UV−visible absorption spectroscopy to monitor the AIBA initiator concentration remaining in the supernatant after centrifugation of the silica sol).

characteristic AIBA absorption at λ_{max} = 368 nm. A Langmuir-type isotherm was obtained as expected (see Figure 10). The maximum adsorbed amount of AIBA was determined to be 3.48 mg g^{-1}, which equates to 0.028 mg m^{-2}. This should be compared to a value of 2.0 mg g^{-1} (or 0.050 mg m^{-2}) reported by Luna-Xavier and co-workers[13] for AIBA adsorbed onto an aqueous 68 nm silica sol (Klebosol 30N50). Presumably, these differing values simply reflect differences in surface charge density and/or hydroxyl content for the two types of silica sol. Such differences in surface charge density between aqueous and alcoholic silica sols are clearly evident in zeta potential measurements, as reported by Percy et al.[1,21] Under the chosen polymerization conditions, we calculate that the AIBA concentration is approximately three times greater than the minimum amount required for monolayer coverage (this assumes no temperature dependence for the extent of adsorption; this is probably not correct, but it would be very difficult to determine the AIBA adsorption isotherm at 60 °C, because the AIBA decomposes at this temperature). Thus the silica particles are most likely completely coated with initiator and excess initiator is also present in solution. It is also noteworthy that, on addition of the cationic AIBA initiator, there is a reduction in zeta potential from −47 to −15 mV (for the MA-ST silica sol at pH 7 diluted in water before and after initiator addition). However, there is no visible flocculation of the silica sol in the presence of this AIBA initiator and there is no significant increase in the mean sol diameter, as judged by DLS studies. Given the significant proportion of adsorbed AIBA initiator, some degree of surface polymerization probably occurs, which should favor more efficient silica incorporation. Nevertheless, it is difficult to confirm that surface polymerization is actually essential for the formation of colloidally stable nanocomposite particles.

4.2.3. Influence of Initiator Concentration. Given the extent of AIBA adsorption onto the silica sol, the effect of varying the initiator concentration was investigated. In the polymerizations conducted so far, approximately 11.5 mg of initiator was used per gram of silica, which equates to more than three times the maximum adsorbed amount of AIBA determined from the adsorption isotherm (i.e., 3.5 mg per gram of silica). This protocol inevitably leads to a

substantial fraction of soluble initiator. Therefore, two additional syntheses were carried out using either 1.5 mg of AIBA per gram of silica (corresponding to approximately 40% of the amount of AIBA required for maximum coverage, see entry 6 in Table 2) or 3.25 mg of AIBA per gram of silica, which is just below the maximum possible amount of initiator (to ensure that no free initiator is present in solution; see entry 7 in Table 2). These reduced initiator concentrations also led to the formation of colloidally stable polystyrene−silica nanocomposite particles. Moreover, the silica contents (and therefore the silica incorporation efficiencies) were somewhat higher than for polystyrene−silica nanocomposite particles prepared at the original higher initiator concentration. Silica contents were 18% at 11.5 mg g^{-1} (entry 4 in Table 2), 21% at 1.5 mg g^{-1} (entry 6 in Table 2) and 24% at 3.25 mg g^{-1} (entry 7 in Table 2), which correspond to silica incorporation efficiencies of 26, 30, and 37%, respectively. Furthermore, the weight-average particle diameter also decreased from 362 nm (for 11.5 mg g^{-1} initiator) to 262 nm (1.5 mg g^{-1} initiator) and slightly broader size distributions were obtained when less initiator was used, as judged by DCP. This smaller mean particle diameter is best explained by the lower rates of polymerization obtained at reduced initiator concentrations.[39]

4.2.4. Influence of Silica Sol Concentration. For the synthesis of silica-stabilized polystyrene latex prepared with a nonionic AIBN initiator, it was shown that variation of the silica sol concentration directly influences the mean particle size of the resulting particles. The effect of varying the silica sol concentration from 4 to 24 w/v % was also investigated in the case of polystyrene−silica nanocomposites (entries 8−10 in Table 2). In contrast to the silica-stabilized polystyrene latex particles, the mean particle diameters vary only slightly between 362 and 322 nm. Thermogravimetric analysis reveal that the final silica contents of 24−25 wt % were also independent of the initial silica sol concentration. This is also reflected in the silica sol incorporation efficiency, which in the case of the lowest initial silica sol concentration of 4 w/v % was as high as 72% (entry 10 in Table 2).

This set of experiments provided some interesting results. The final silica content and, to some extent, the particle size of the polystyrene−silica nanocomposites were essentially independent of the initial silica sol concentration. Thus it seems that, above a certain value, higher silica sol concentrations have little effect on the properties of the final polystyrene−silica nanocomposite particles. The polymerization appears to proceed up to a mean particle diameter of around 330 nm and a silica content of approximately 24% is attained, regardless of the level of excess silica sol. Currently, we have no satisfactory explanation for these limiting conditions, although we note that Percy et al. reported that poly(4-vinylpyridine)−silica particle syntheses were similarly insensitive to systematic variation of the synthesis parameters.[17]

Comparing entry 9 in Table 2 with the low initiator concentration experiment (entry 7 in Table 2) indicated that identical silica contents and very similar mean particle diameters were obtained in these syntheses. This reproducibility is presumably related to the almost constant initiator/silica mass ratios used in these two protocols. Moreover, the initiator concentration was close to the maximum adsorbed amount (3.8 mg g^{-1} and 3.25 mg g^{-1}, respectively) in both cases.

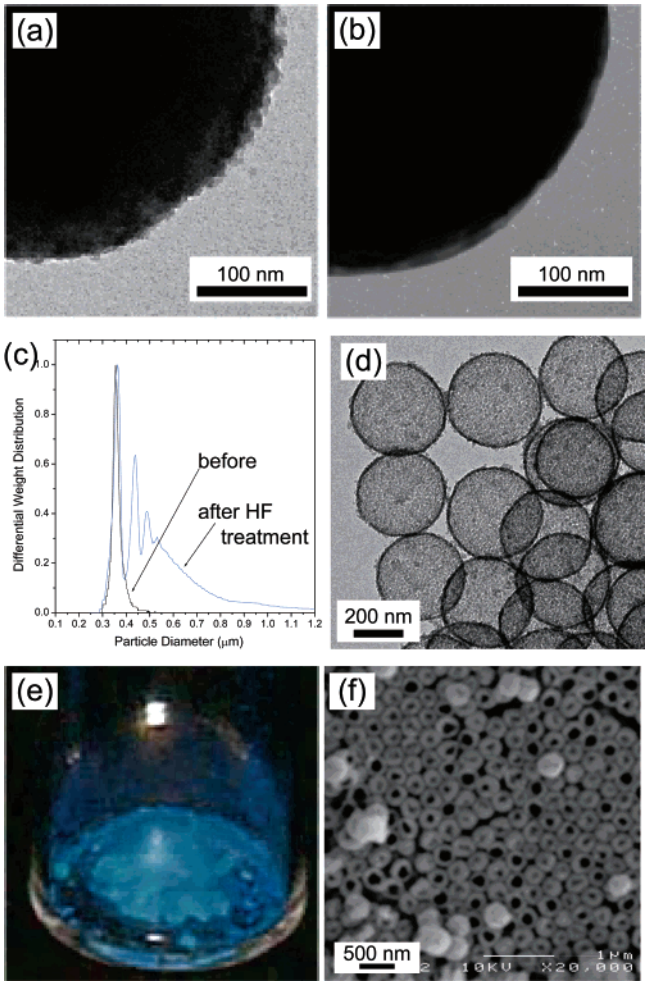

Figure 11. Selected TEM images and DCP curves obtained for polystyrene−silica nanocomposites (a) before and (b) after treatment with 20% HF, which leads to digestion of the silica sol and flocculation of the remaining polystyrene particles, as confirmed by the disk centrifuge particle size distribution curves shown in (c); (d) calcination at above 550 °C leads to complete pyrolysis of the polystyrene component, leading to the formation of hollow silica particles; (e) the digital photograph shows the blue color observed when these silica particles are viewed on a dark background after calcination; (f) the corresponding SEM image of this calcined sample. Images a−c were obtained for entry 4 in Table 2, whereas images d−f were obtained for entry 7 in Table 2.

4.2.5. Particle Morphology. Aqueous electrophoresis measurements of the three types of nanocomposite particles indicated negative zeta potentials over the whole pH range, as observed for the three pristine silica sols. This is illustrated for the nanocomposite synthesis conducted using the 22 nm silica sol, see Figure 5. This suggests that the surface of the nanocomposite particles is silica-rich. This finding is corroborated by the following observations. Treatment of one of the nanocomposites prepared with the 22 nm silica sol (entry 4 in Table 2) with excess 20% aqueous HF solution ensured complete digestion of the silica sol component but left the polystyrene component untouched. Subsequent

(39) Lovell, P. A.; El-Aasser, M. S. *Emulsion Polymerisation and Emulsion Polymers*; John Wiley & Sons: Chichester, U. K., 1997.

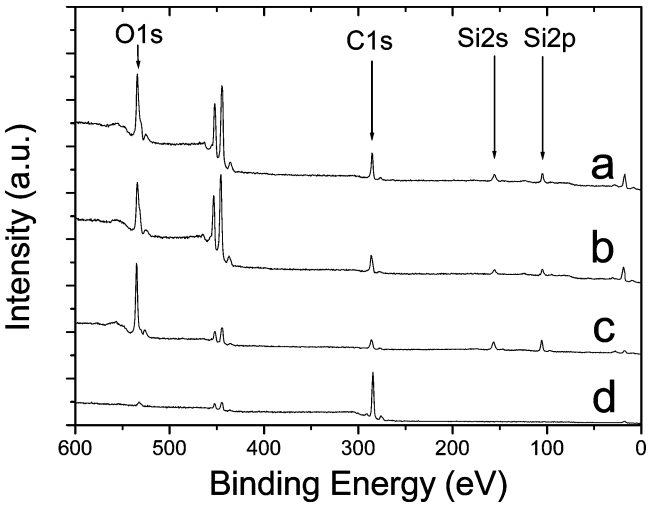

Figure 12. XPS survey spectra of polystyrene−silica nanocomposites prepared via AIBA-initiated alcoholic dispersion polymerization in the presence of three commercial alcoholic silica sols: (a) 13 nm IPA-ST silica sol in 2-propanol (entry 5 in Table 2), (b) 22 nm MA-ST silica sol in methanol (entry 4 in Table 2), and (c) 13 nm MT−ST silica sol in methanol (entry 3 in Table 2). As a comparison, a survey spectrum recorded for a polystyrene latex prepared in the absence of any silica sol (entry 12 in Table 2) is shown in (d). Given the typical XPS sampling depth of 2−5 nm, these spectra confirm the presence of the silica sol at the surface of the nanocomposite particles.

examination by transmission electron microscopy revealed that the original surface roughness due to the presence of the ultrafine silica particles was replaced with a much smoother particle surface, see images a and b of Figure 11. This digestion of the silica sol was accompanied by a concomitant loss in colloidal stability (i.e., weak flocculation), as judged by both visual inspection and DCP studies (Figure 11c). Moreover, calcination of the same nanocomposite particles at 800 °C led to selective pyrolysis of the polystyrene component, leaving self-supporting hollow silica shells. Thus, these three experiments are consistent with the original polystyrene−silica nanocomposite particles possessing a core−shell morphology. This hypothesis was further confirmed by XPS analysis. Figure 12 shows the survey spectra for the polystyrene−silica nanocomposite particles prepared with the three alcoholic silica sols and also polystyrene latex particles prepared in the absence of any silica sol. Surface Si/C atomic ratios were calculated from the corresponding Si2p and C1s core-line spectra and compared with bulk Si/C atomic ratios calculated from TGA data (see Table 3). The surface Si/C atomic ratio is always at least 1 order of magnitude greater than the bulk Si/C ratio. Given that the typical XPS sampling depth is 2−5 nm, this indicates that the silica sol is located at the surface of the nanocomposite particles. Moreover, comparing the surface silicon compositions of entries 7−9 with that of the pristine silica sols (entries 1−3) suggests that the silica sol occupies 43−75% of the surface of the nanocomposite particles. This range of surface compositions is significantly greater than that calculated for the silica-stabilized latexes (see earlier) and is consistent with approximately monolayer coverage, because 2D packing of the silica particles can only cover 50−60% of the available surface. There are two reasons for the relatively high C1s signal observed by XPS. First, the silica particles contain surface carbon due to unhydrolyzed

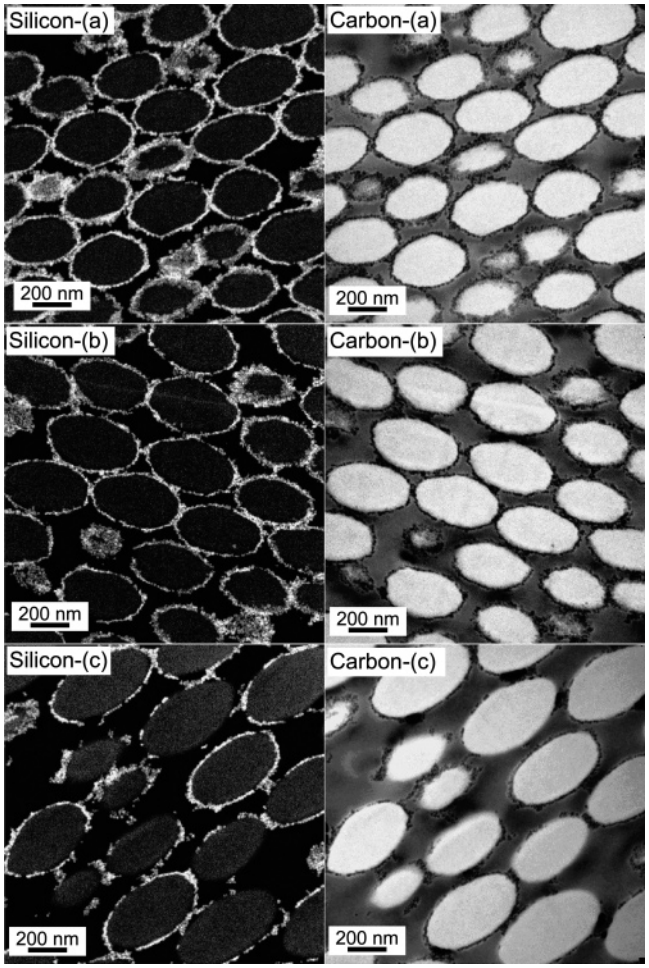

Figure 13. Elemental distribution maps obtained for silicon (left) and carbon (right) from ultramicrotomed polystyrene−silica nanocomposite particles prepared by alcoholic dispersion polymerization using AIBA: (a) nanocomposites prepared in the presence of the MT-ST 13 nm silica sol in methanol (entry 3 in Table 2), (b) MA-ST 22 nm silica sol in methanol (entry 4 in Table 2), and (c) IPA-ST 13 nm silica sol in 2-propanol (entry 5 in Table 2). Silicon is present on the surface of the particles, whereas the core comprises only carbon with no evidence for any silicon. These observations confirm the core−shell morphologies of these nanocomposite particles.

alkoxy groups (see entries 1−3 in Table 3). Second, the inefficient 2D packing of the silica particles leaves 25−57% of the underlying polystyrene still visible on the surface.

The core−shell morphologies of these nanocomposite particles were verified using the ESI/TEM technique in combination with ultramicrotomy, which provided element-specific information at high spatial resolution. In the carbon maps shown in Figure 13, the cross-sectioned particles are easily visualized within the diffuse gray epoxy resin matrix. Bright halos with dark interiors within the gray matrix were observed in the silicon maps. These images confirm that each nanocomposite particle has a well-defined core−shell morphology, consisting of a polystyrene core, containing essentially no silica particles, surrounded by a thin monolayer shell of ultrafine silica particles. The somewhat elliptical particle geometry observed in the TEM images shown in Figure 13 is an artifact due to sample shearing during ultramicrotomy and does not reflect the original particle geometry.

Conventional oven-drying of a polystyrene−silica nanocomposite (entry 7 in Table 2) at 60 °C for 24 h results in

a white nanocomposite powder, as expected. However, calcination at 800 °C pyrolyzes the polystyrene component completely, leaving the incombustible silica as a powder. This remaining silica appears yellowish when viewed in transmitted light, but a distinctive blue color is observed if the silica is placed on a dark background, see Figure 11e. TEM studies of the calcined silica confirmed the presence of hollow particles formed by partial fusion of the ultrafine silica sol during calcination due to dehydration of the surface silanol groups (see Figure 11f). SEM studies confirm that most, if not all, of these hollow silica particles contain defects or holes, presumably caused by loss of organic volatiles during the polystyrene pyrolysis. We believe that this unexpected blue coloration is due to the hollow silica diameter being comparable to approximately half the wavelength of visible light[7] (see entries 4 and 7 in Table 2 for the original polystyrene−silica nanocomposite diameters).

4.2.6. Anionic ACVA Initiator. Performing dispersion polymerization syntheses using an anionic ACVA initiator in the presence of an alcoholic silica sol only led to precipitation of amorphous polystyrene, with rather little evidence for particle formation (see the Supporting Information). This underlines the importance of a strong electrostatic interaction between the initiator/growing polymer chain and the anionic silica sol for successful nanocomposite formation.

4.2.7. Control Experiments. Four control experiments were conducted by polymerizing styrene in methanol or 2-propanol using either AIBA or ACVA initiators in the absence of any silica sol. Only those dispersion polymerizations conducted in methanol led to the formation of colloidally stable (presumably charge-stabilized) polystyrene latexes. Polymerizations in 2-propanol merely led to precipitation of amorphous polystyrene, with no evidence of particle formation.

GPC analyses of the polystyrene extracted from a polystyrene−silica nanocomposite prepared in methanol (entry 4 in Table 2) and the corresponding charge-stabilized polystyrene latex obtained in the control experiment conducted under identical conditions in the absence of silica (entry 12 in Table 2) are shown in the Supporting Information (see Table S1). The molecular weight and polydispersity obtained for the polymeric component of the nanocomposite (M_w = 423 000; M_w/M_n = 5.55) are comparable to that obtained for the charge-stabilized polystyrene latex (M_w = 456 000; M_w/M_n = 4.44). Thus the presence of the silica sol appears to have little, if any, effect on the styrene polymerization. The molecular weight of the polymeric component of the polystyrene−silica nanocomposite prepared in 2-propanol is a little higher (M_w = 518 000), but this is likely to be within experimental reproducibility. These nanocomposite M_w values are significantly higher than those obtained for the silica-stabilized polystyrene latexes (see earlier).

Typical particle growth curves were obtained by DLS studies of the polymerization of styrene in the presence of the 22 nm methanolic MA-ST silica sol initiated by either AIBN (entry 4 in Table 1) or AIBA (entry 4 in Table 2). In a control experiment, a particle growth curve was also obtained for a cationic polystyrene latex prepared with AIBA in the absence of any silica sol (entry 12 in Table 2). For the AIBN-initiated polymerization, the final particle diameter was attained after around 12 h. In contrast, no further change in particle diameter was observed after only 3−4 h for the two styrene polymerizations conducted with the AIBA initiator. This difference simply reflects the differing half-lives for these two initiators at 60 °C (approximately 440 min for AIBA and around 1300 min for AIBN). More importantly, no significant differences were observed for the particle growth curves obtained from the two AIBA-initiated polymerizations conducted in the presence and absence of the silica sol. This suggests that if surface polymerization does occur under these conditions, it does not appear to affect the overall kinetics of polymerization.

5. Conclusions

Alcoholic dispersion polymerization can be used to prepare both silica-stabilized polystyrene latex particles and polystyrene−silica nanocomposite particles using alcoholic ultrafine silica sols as the sole stabilizer. When a nonionic AIBN initiator was used, polymerizations of styrene conducted in either methanol or 2-propanol led to micrometer-sized, silica-stabilized polystyrene latexes. These latexes had very low silica contents (no more than 1.1%). Nevertheless, the silica sol is located exclusively at the particle surface and is solely responsible for the colloidal stability. Decreasing the silica sol concentration in the polymerization mixture leads to an increase in particle diameter, as expected. The silica incorporation efficiency was typically very low in such syntheses.

Similar polymerizations conducted using a cationic AIBA initiator led to the formation of submicrometer-sized polystyrene-silica nanocomposite particles. Mean particle diameters varied between 262 and 464 nm and silica contents ranged between 13 and 29 wt %, depending on the precise reaction conditions and the silica sol type used. Variation of the silica sol concentration and initiator concentration, as exemplified for the 22 nm silica sol, has surprisingly little influence over both the final silica content and particle diameter. XPS and ESI/TEM studies confirm well-defined core−shell morphologies for these nanocomposite particles (i.e., polystyrene cores and thin silica shells). Hollow silica particles can be formed after calcination, suggesting that the surface layer of silica nanoparticles is reasonably contiguous.

Acknowledgment. The authors thank Dr. J. Du for assistance with TEM studies, Mr. R. Ducker for his assistance with the HF etch experiments, Miss T. Colburn for running some additional XPS spectra, and Mr. J. Madsen for the GPC measurements. The University of Sheffield is acknowledged for a PhD studentship for A.S., and S.P.A. is the recipient of a 5-year Royal Society-Wolfson Trust Research Merit Award. Nissan Chemicals (USA) is thanked for donating the alcoholic silica sols.

Supporting Information Available: SEM image of amorphous polystyrene prepared as a macroscopic precipitate using the anionic ACVA initiator, particle growth curves determined by dynamic light scattering, GPC analysis of four polystyrene samples extracted from nanocomposite particles, and three reference polystyrene latex samples. This information is available free of charge via the Internet at http://pubs.acs.org.

CM062314C